Supporting Information

Keller et al. 10.1073/pnas.0906361106

SI Text

Animals. Male C57BL/6 mice were obtained from Bundesinstitut für Risikobewertung, and male C57BL/6 adrenalectomized mice were purchased from Charles River Laboratories (www.criver-.com/SiteCollectionDocuments/rm_ss_r_adrenalectomy.pdf). PER2::LUC mice on a C57BL/6 background were kindly provided by J. S. Takahashi (1). *Per1*::*luc* rats (kind gift of Hajime Tei) (2) were raised and housed at Hilltop Animal Facility of Washington University (St. Louis, MO).

Animals were maintained individually in cages with continuous access to food, water and a running wheel. All procedures were in accordance with institutional guidelines and the requirement of the state authority for animal research conduct. Mice and rats were housed in a 12-h light/12-h dark (LD) cycle for at least 2 weeks before transfer to constant darkness (DD).

Quantitative RT-PCR. Spleen and inguinal lymph nodes of 8- to 10-week-old male C57BL/6 mice were harvested in 3- or 6-h intervals over the course of the first 2 days in DD to exclude direct effects of light on gene expression. Total RNA was isolated with RiboPure (Ambion), from spleen or with RNeasy kit (Qiagen), from lymph nodes, and then reverse transcribed to cDNA by using SuperScript II (Invitrogen) and random hexamer primers (MWG). Spleen and lymph nodes: *Per2* and *Rev-Erbα* transcript levels were determined by using TaqMan quantitative PCR. Primers and 5′-FAM-3′-TAMRA-labeled probes were designed according to the guidelines of the Primer Express 2.0 software (Applied Biosystems). Primer and probe sequences: *Gapdh*: forward TGTGTCCGTCGTGGATCTGA, reverse CCTGCTTCACCACCTTCTTGA, probe CCGCCTGGAGAAACCTGCCAAGTATG, *Rev-Erbα*: forward AGGTGGTAGAGTTTGCCAAACAC, reverse CACCATCAGCACCTCAAAGGT, probe TCCGTGACCTTTCTCAGCACGACCA, *Per2*: forward ATGCTCGCCATCCACAAGA, reverse GCGGAATCGAATGGGAGAAT, probe ATCCTACAGGCCGGTGGACAGCC. Validation of gene chip expression profiles from peritoneal macrophages (Figs. 4 and 5): total RNA was prepared by using the RNeasy Mini kit (Qiagen) and reverse transcribed to cDNA with Reverse Transcriptase (Fermentas). Quantitative PCRs were performed in triplicate with SYBR green fluorescence assays using mouse QuantiTect Primer assays (Qiagen) and analyzed with ABI Prism 7000 Sequence Detection System (Applied Biosystems). The transcript levels for clock genes were normalized to *Gapdh* mRNA according to the $2^{-\mathrm{ddCt}}$ method (3) and additionally to mean expression levels (Figs. 4 and 5) or to minimum expression (Fig. 1).

Real-Time Bioluminescence Monitoring. Spleen and lymph node: Male PER2::LUC mice (1) and a *Per1:luc* rat (2) were entrained to a LD cycle. At the age of 2 months, mice were killed 2 hours before the end of the light period. A small piece of spleen and two superficial inguinal lymph nodes were cultured individually on Millicell membranes (Millipore) with 1 mL of DMEM (Sigma) supplemented with 0.1 mM beetle luciferin (Promega) as previously described (4). Macrophages were harvested by peritoneal lavage with sterile, ice-cold PBS (PBS, 3–4 mL). Cells were collected by centrifugation (300 × *g*, 10 min, RT), and the pellet was resuspended in DMEM supplemented with 10% serum and 0.1 mM luciferin (Promega). Cells were cultured in Petri dishes and finally covered with lids, sealed with grease, and placed in light-tight boxes using a single photomultiplier tube (Hamamatsu Photonics) at 36.5 °C in the dark. Bioluminescence was recorded in 1-min bins for at least 6 days.

FACS Analysis. Spleen cells (i.e., splenocytes—mononuclear white blood cells extracted from splenic tissue) were derived as follows: Spleens from C57BL/6 mice were harvested, cut into pieces, and passed through a cell strainer (BD Biosciences). Red blood cell lysis was performed with distilled water. Splenic B cells, T cells, and macrophages were labeled with anti-mouse CD11b, anti-mouse CD14, anti-mouse CD19, and anti-mouse CD90.2 (BD Biosciences) on ice. Cells were washed twice with ice-cold FACS buffer (PBS, 1% FCS, 0.05% sodium azide), fixed with 1% paraformaldehyde in PBS and subsequently analyzed on FACSscan flow cytometer (Becton Dickinson) using CellQuest software.

Sort control: MACS-sorted $CD11b^+$ peritoneal cells were labeled with anti-mouse CD11b (Miltenyi Biotec), anti-mouse CD19 (BD Biosciences), and anti-mouse CD14 (eBiosciences) antibodies according to manufacturer instructions and consecutively analyzed with a FACS canto II (BD). Samples with <90% CD11b-positive cells were excluded from further processing.

Cell Sorting. Peritoneal cells from C57BL/6 or PER2::LUC mice were collected by lavage of the peritoneal cavity with 2 mL of ice-cold PBS. Macrophages were isolated based on the expression of the CD11b surface marker by using anti-mouse CD11b microbeads (Miltenyi Biotec) and a magnetic separation system (autoMACS; Miltenyi Biotec). A small fraction of positive CD11b sorted cells were purity analyzed by FACS (see above).

LPS Stimulation and ELISA. ***Ex vivo LPS stimulation experiment.*** Spleens of 8- to 10-week-old male C57BL/6 mice were harvested at regular 4-h intervals on the first day in DD and processed to a single-cell suspension. The cells were cultured in RPMI medium 1640 containing 10% FCS and immediately treated with 5 μg/mL of a highly pure lipopolysaccharide preparation (LPS, Alexis, from *E. coli* serotype R515) for 4 h. Cell-free supernatants were harvested, frozen at −20 °C, and analyzed at the end of the time-series.

In vitro LPS stimulation experiment. Primary splenic and peritoneal macrophages were collected, resuspended in endotoxin-free media (RPMI medium 1640, 10% FBS) and cultured at 37 °C, 5% CO_2. Twenty-four hours after seeding, cells were treated with LPS (3 μg/mL) for 4 h. TNF-α and IL-6 contents in the supernatant were analyzed by ELISA according to the manufacturer's recommendations. TNF-α ELISA was purchased from Biosource and IL-6 ELISA from eBioscience.

Transcriptional Profiling (Microarray Analysis). C57BL/6 mice were entrained to a LD cycle and then transferred to DD. The first day in DD, peritoneal macrophages from four mice per time point were collected and magnetically sorted (see *Cell Sorting* for details) every 4 h. Total RNA was isolated by using RNeasy Mini kit (Qiagen). Integrity and amount of total RNA was analyzed by using an Agilent 2100 Bioanalyzer (Agilent). RNA of three mice per sampling time was pooled in equal amounts (48 ng/μL). Synthesis of cDNA, amplification, labeling, and hybridization were performed by the Labor für Funktionelle Genomforschung (LFGC, Charité, Berlin), by using GeneChip Mouse Gene 1.0 ST arrays (Affymetrix). Data acquisition and primary analysis–acquisition and quantification of array images as well as primary data analysis were performed by using the Affymetrix software

packages: Microarray Suite version 5.0 and Data Mining Tool version 2.0. Circadian expressed genes were identified by using the CircWaveBatch v3.3 software (R. A. Hut) (5) with a cutoff *P* value of 0.05 and period length restricted to 24 h.

Statistical Analysis. Time-series data on cytokine secretions were analyzed with CircWave v1.4 software (R. A. Hut) (5) by using a linear harmonic regression fit with an assumed period of 24 h (www.rug.nl/biologie/onderzoek/onderzoekgroepen/chronobiologie).

Local False-Discovery Rate (lfdr). The lfdr estimates the fraction of false-positive tested datasets at a given *P* value from a larger set of data. To that end, *P* values of genes with a average expression value of ≥50 from the microarray analysis were analyzed by using the "R" package (www.r-project.org/) "fdrtool" (K. Strimmer, http://strimmerlab.org/software/fdrtool/). Therein, the proportion of null values and the parameters of the null distribution are adaptively estimated from the data. For a detailed description of the method and package, see refs. 6 and 7.

1. Yoo SH, et al. (2004) PERIOD2::LUCIFERASE real-time reporting of circadian dynamics reveals persistent circadian oscillations in mouse peripheral tissues. *Proc Natl Acad Sci USA* 101:5339–5346.
2. Yamazaki S, et al. (2000) Resetting central and peripheral circadian oscillators in transgenic rats. *Science* 288:682–685.
3. Livak KJ, Schmittgen TD (2001) Analysis of relative gene expression data using real-time quantitative PCR and the 2(-Delta Delta C(T)) Method. *Methods* 25:402–408.
4. Abe M, et al. (2002) Circadian rhythms in isolated brain regions. *J Neurosci* 22:350–356.
5. Oster H, Damerow S, Hut RA, Eichele G (2006) Transcriptional profiling in the adrenal gland reveals circadian regulation of hormone biosynthesis genes and nucleosome assembly genes. *J Biol Rhythms* 21:350–361.
6. Strimmer K (2008) A unified approach to false discovery rate estimation. *BMC Bioinformatics* 9:303.
7. Strimmer K (2008) fdrtool: A versatile R package for estimating local and tail area-based false discovery rates. *Bioinformatics* 24:1461–1462.
8. Panda S, et al. (2002) Coordinated transcription of key pathways in the mouse by the circadian clock. *Cell* 109:307–320.
9. Storch KF, et al. (2002) Extensive and divergent circadian gene expression in liver and heart. *Nature* 417:78–83.
10. Nagoshi E, et al. (2004) Circadian gene expression in individual fibroblasts: Cell-autonomous and self-sustained oscillators pass time to daughter cells. *Cell* 119:693–705.

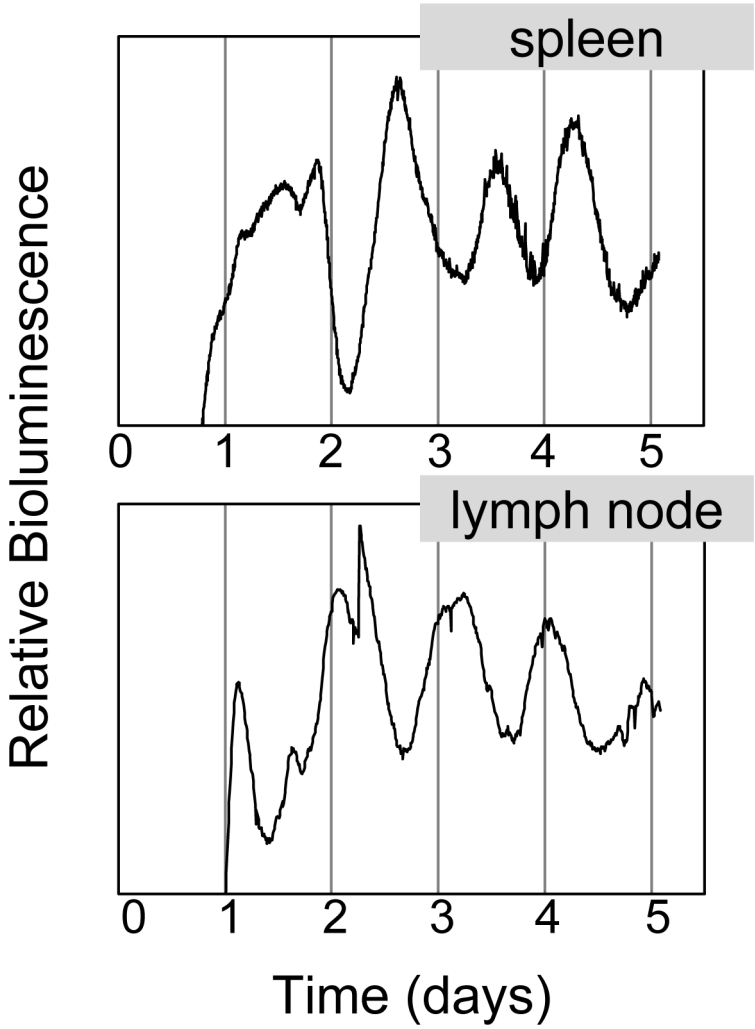

Fig. S1. Circadian, tissue autonomous oscillations in spleen and lymph nodes from a *Per1:luc* rat. A piece of spleen and two superficial inguinal lymph nodes were cultured individually and light emission was counted in 1-min bins for >5 days. Raw data were divided by a 24-h running average to eliminate trends in luminescence decay. Note, that damping of circadian rhythms in these tissue explants is believed to be caused by internal desynchronisation of self-sustained clock cells (10).

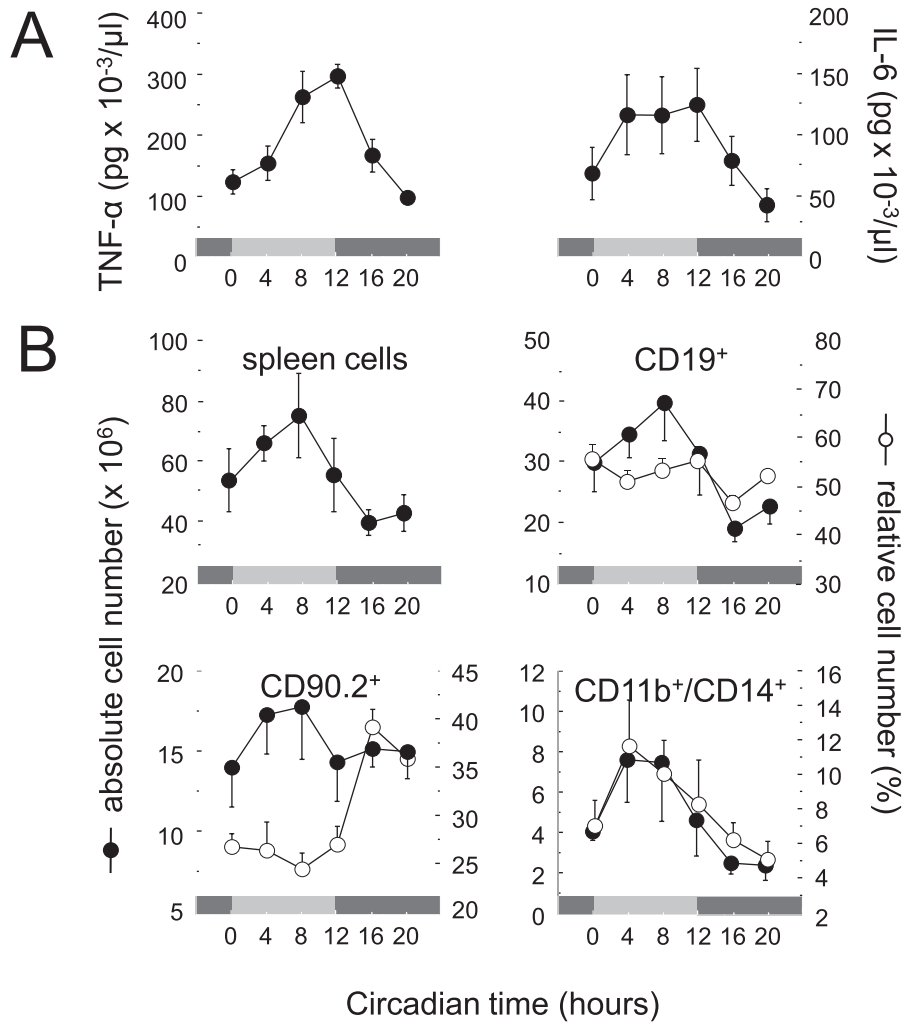

Fig. S2. Cytokine secretion of TNF-α and IL-6 is regulated by an intrinsic clock. (*A*) Circadian modulation of LPS-induced cytokine response is independent of systemic cortisol. Spleens from adrenalectomized (ADX) C57BL/6 mice were harvested and analyzed similar to Fig. 2. TNF-α and IL-6 cytokine secretion was determined by ELISA. Circadian oscillations are statistically significant as analyzed with CircWave (mean values $\pm$ SEM, $n = 4$–5, $P < 0.001$ and $P < 0.05$ for TNF-α and IL-6, respectively). (*B*) Cellular composition of the spleen in ADX mice. Same samples as in *A* were analyzed by using cell-counting chamber and flow cytometry. CD19, CD90.2 and CD11b/CD14 were used as characteristic surface markers of B cells, T cells, and monocytes/macrophages, respectively.

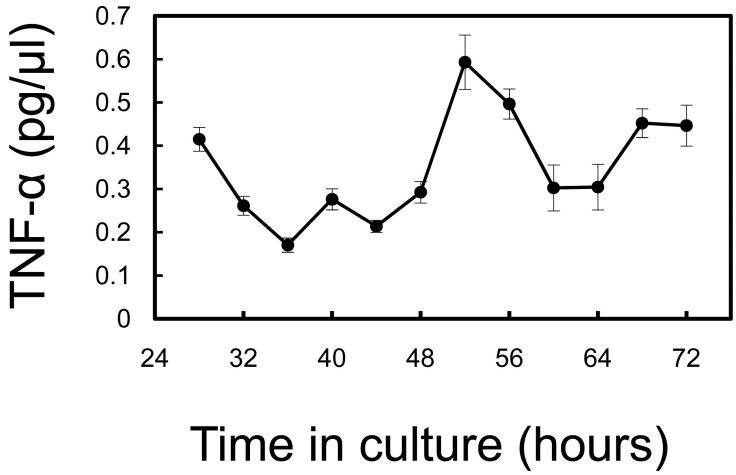

Fig. S3. Circadian cytokine secretion upon challenge with bacterial endotoxin in peritoneal macrophages. TNF-α secretion upon LPS stimulation is regulated by a local, cell intrinsic clockwork. Peritoneal macrophages from C57BL/6 mice were harvested, pooled, and plated for cell culture on multiple microtiter plates. Eight to ten wells per time point were stimulated with LPS, and supernatants were collected 4 h later. TNF-α concentrations in supernatants were analyzed by ELISA (mean values $\pm$ SEM, $n = 8$-10). Statistical analysis using CircWave revealed a significant circadian pattern ($P < 0.01$).

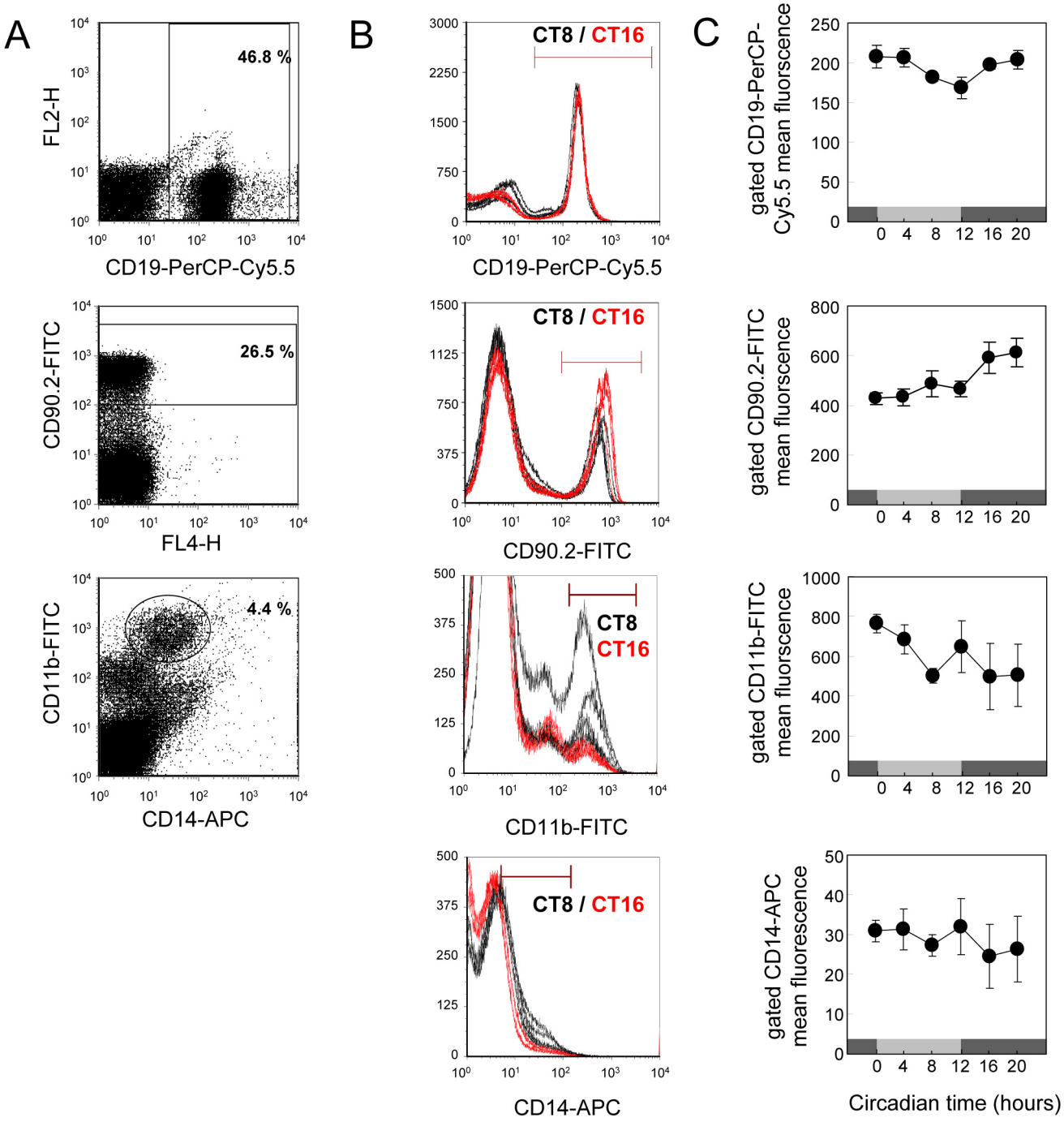

Fig. S4. Representative FACS analysis of spleen cells derived from C57BL/6 mice. (*A*) FACS analysis on the circadian pattern of spleen cell composition (see also Fig. 2). Spleens of 8- to 10-week-old male C57BL/6 mice were harvested at regular 4-h intervals and the frequency of B cells, T cells, and monocytes/macrophages was determined by FACS analysis. Shown are gate settings for B cells (CD19+), T cells (CD90.2+), and monocytes/macrophages (CD11b+/CD14+) with representative frequency numbers. (*B* and *C*) Surface marker expression of analyzed splenocyte subpopulation is not regulated in a circadian fashion. To compare surface marker expression at peak and trough times of relative (CD90.2, CD11b/CD14) and absolute (CD19) cell numbers, we generated overlays of the respective histograms (*B*). Quantified mean fluorescence intensities of gated (see *A* and *B*) cell populations do not change significantly throughout the circadian day (*C*).

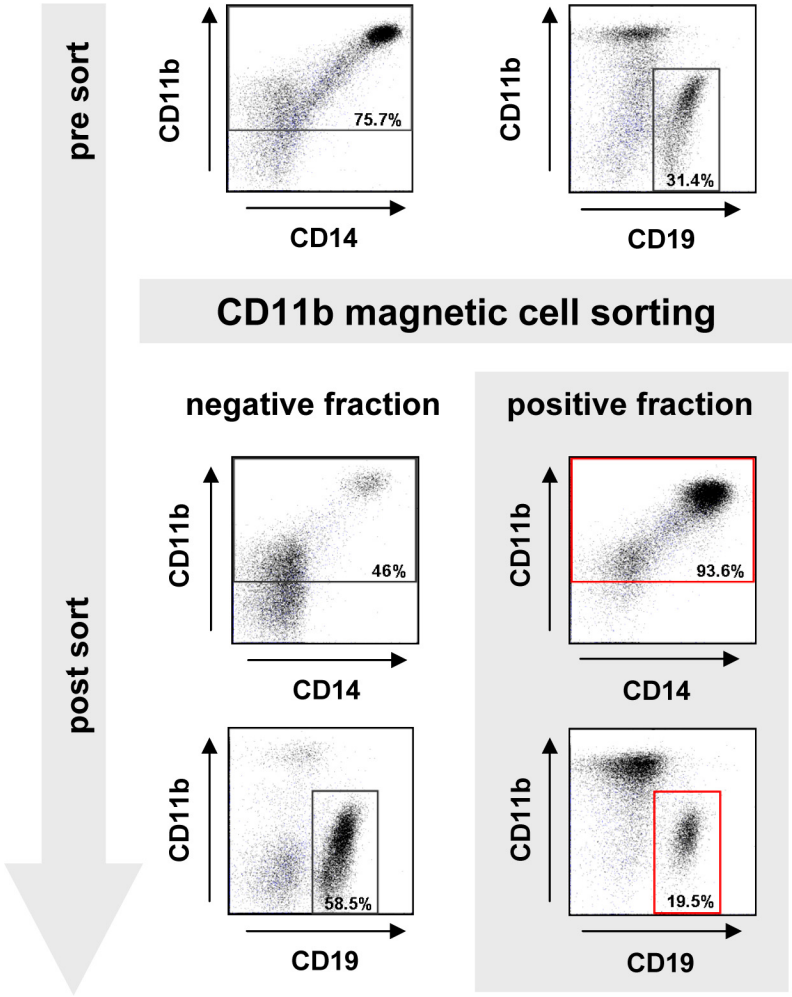

Fig. S5. Schematic representation of MACS sort strategy on peritoneal cells derived from C57BL/6 mice. Peritoneal macrophages designated to microarray transcriptional profiling were CD11b-MACS sorted and subsequently analyzed for sorting efficiency and purity.

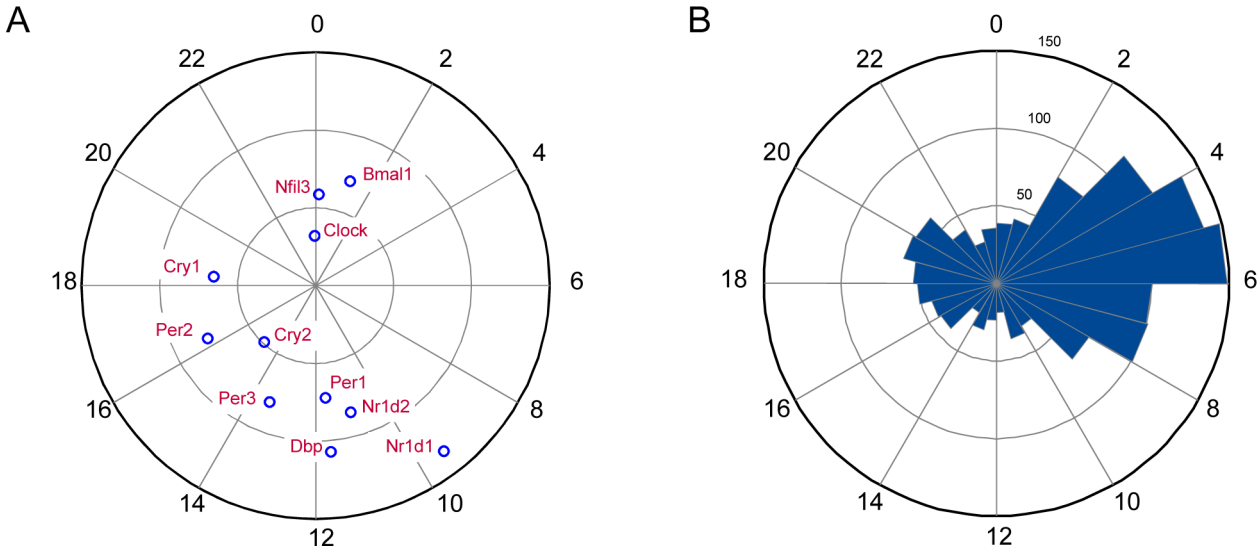

Fig. S6. Phase relations of circadian expressed genes in peritoneal macrophages. (*A*) Peak phases and relative amplitudes of circadian clock genes were extracted from microarray dataset. Transcriptional activators like Clock and Bmal1 are expressed in antiphase to their inhibitors Pers, Crys, and Nr1d1. (*B*) Peak phase distribution of 1,403 circadian transcripts indicates that these genes were preferentially expressed between CT3 and CT8.

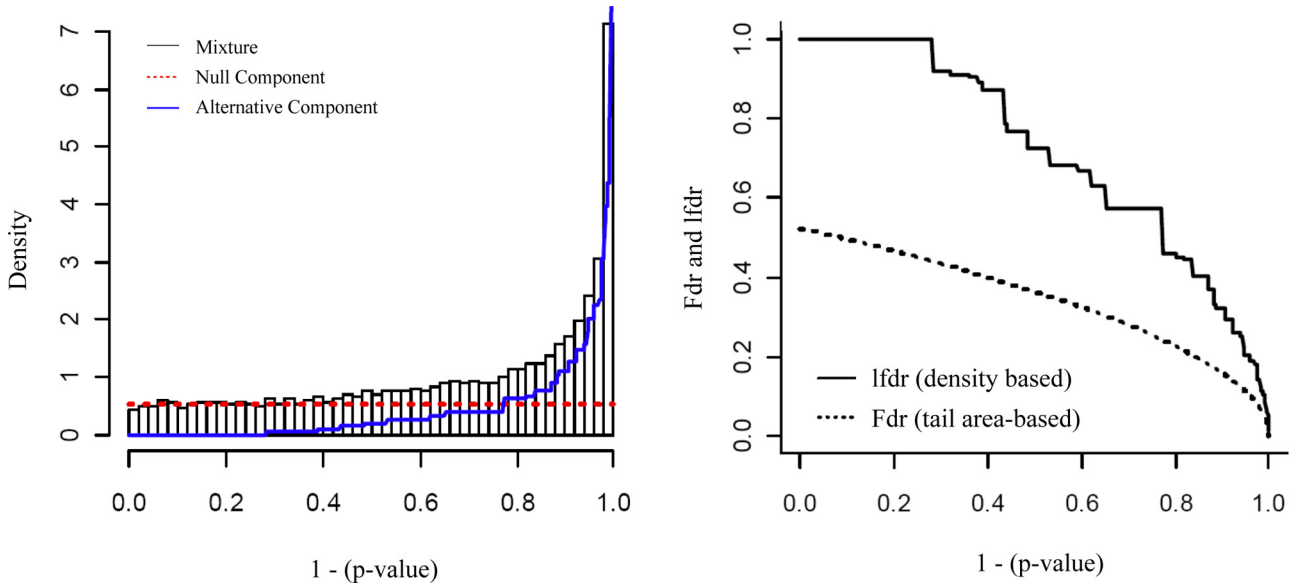

Fig. S7. Statistical analysis of circadian transcriptional profiling in peritoneal macrophages was corrected for multiple testing via the estimation of lfdrs. Microarray data were analyzed for circadian patterns with CircWaveBatch (see *Materials and Methods* for details) and subsequently controlled for multiple testing errors by using the ''R'' package ''fdrtool'' (6, 7). Density normalized distribution of *P* values from datasets with a mean expression value >50 (*Left*) visualizes the estimation of the null component as a measure of truely negative (i.e., noncircadian) datasets (eta0 = 0.5388). Conversely, the alternative component depicts the estimated density of truely positive (i.e., circadian) datasets at a given *P* value. From this, the ratio of truly negative to positive-tested datasets (i.e., the false-discovery rate) can be calculated for a specific *P* value (lfdr) (*Right*).

Table S1. Peak phases and amplitudes of circadian genes in peritoneal macrophages compared with other tissues

	Peritoneal macrophages			SCN*	Liver*†	Heart†
Gene symbol	P‡	Amplitude¶	Peak-phase [h]	Peak-phase [h]	Peak-phase [h]	Peak-phase [h]
Nr1d1§	≤0.01	5.38	9.5	16.3	7.9/–	
Dbp§	≤0.01	4.29	11.7		–/7.5	8.1
Nr1d2	≤0.0001	3.37	11.0	14.3	10.6/–	
Per2§	≤0.0001	3.22	16.3	11.2	15.4/14.6	10.9
Per3	≤0.0001	3.08	13.4			
Per1§	≤0.05	2.89	11.7		–/11.2	8.2
Arntl§	≤0.0001	2.82	1.2	2.4	–/20.8	22.8
Cry1§	≤0.0001	2.62	18.3		–/17.3	
Nfil3	≤0.0001	2.34	0.1		0.9/20.0	20.8
Cry2§	≤0.01	1.95	14.8			
Clock§	≤0.05	1.24	9.2			

*Data from ref. 8.
†Data from ref. 9.
‡*P* values have been determined by using CircWave Batch (5).
§Circadian gene transcription was confirmed by quantitative RT-PCR analysis (Fig. 4).
¶Amplitudes have been determined by calculating the peak-to-trough ratios from fitted sine waves (CircWave Batch).

Table S2. Circadian control of gene transcription within the LPS response pathway

Gene symbol	Synonym	$P^{\dagger}$	Lfdr[‡]	Amplitude	Phase [h]
Jun[§]	c-jun, AP-1	≤0.0001	0.01	1.61	13.7
Adam17[§]	Tace, CD156b	≤0.0001	0.01	1.22	2.6
Cd180[§]	Rp105*, Ly78	≤0.0001	0.01	1.70	0.5
Sfpq	PSF	≤0.001	0.02	1.29	14.1
Nfkbia[§]	IκBα*	≤0.01	0.04	1.37	15.8
Ly86[§]	MD-1*	≤0.01	0.04	1.34	0.8
Map2k1[§]	Mek1*, Prkmk1	≤0.01	0.05	1.17	11.3
Traf3	CAP-1, CD40bp	≤0.01	0.05	1.27	11.6
Elavl1[§]	HuR	≤0.01	0.05	1.32	10.2
Fos[§]	c-fos	≤0.01	0.05	1.75	12.9
Mapk3[§]	Erk1*, Prkm3	≤0.01	0.06	1.28	0.8
Map2k7[§]	MKK7	≤0.01	0.06	1.42	1.4
Tank	I-TRAF	≤0.01	0.06	1.36	5.3
Rela	p65 NFκB, p65	≤0.05	0.09	1.19	20.2
Ikbkb	IKK2, IKKβ	≤0.05	0.09	1.18	11.8
Ripk1	Rip1*	≤0.05	0.09	1.11	22.7
Mapk14	p38*, Crk1	≤0.05	0.11	1.21	15.8
Cd14		≤0.05	0.11	1.24	21.9
Map2k3	Mek3*, MKK3	≤0.05	0.15	1.39	14.7
Ccl3	MIP1-α*	≤0.05	0.15	1.65	1.3
Atf2	Creb2, CRE-BP	≤0.05	0.15	1.20	22.8
Mknk2	Mnk2*, Gprk7	≤0.05	0.16	1.38	17.4
Mapkapk2	MK2*, Rps6kc1	≤0.05	0.17	1.17	15.7
Irf3		≤0.05	0.17	1.12	4.5
Mef2c	Mef2	≤0.05	0.17	1.28	1.6
Tial1	mTIAR	≤0.05	0.17	1.17	15.2

Selected datasets from whole-genome transcriptional profiling using microarray analysis (see *Methods*).

*Synonyms used in Fig. 5*A*.

[†]*P* values have been determined by using CircWave Batch (5).

[‡]For a detailed description of local false discovery rate (lfdr) estimation see refs. 6 and 7.

[§]Circadian gene transcription was confirmed by quantitative RT-PCR analysis (Fig. 5).